Int. J. Electrochem. Sci., 11 **(2016)** 140 - 153

International Journal of
ELECTROCHEMICAL
SCIENCE
www.electrochemsci.org

Electrochemical Behavior and Compositions of Passive Films of Amorphous Ni-P Coating in Acidic Environment

Guanlin Zhao[1], *Yong Zou*[1,*], *Sui Jinwen*[2], *Kenji Matsuda*[3], *Zengda Zou*[1], *Jie Chen*[1]

[1]Key Lab of Liquid Structure and Heredity of Materials, Ministry of Education, Shandong University, Jinan 250061, China
[2]State Grid Shandong Electric Power Maintenance Company, Jinan 250118, China
[3]Department of Materials Science and Technology, Faculty of Engineering, University of Toyama, Toyama, 930-8555, Japan
[*]E-mail: yzou@sdu.edu.cn

Received: 19 October 2015 / *Accepted:* 10 November 2015 / *Published:* 1 December 2015

Amorphous Ni-P coating without pores was prepared by electroless plating. The electrochemical behavior of the as-plated Ni-P coating was investigated by potentiodynamic testing in 5 wt. % sulfuric acid solution. Results indicated that the high-phosphorus Ni-P coating has a passivation region in the acid solution. The passive films possessed n-type semiconductor characteristic basing on the Mott-Schottky analysis. Different anodic potentials and polarization time affect the passive films properties. The passive film shows the best corrosion resistance when the potentiostatic potential was 0.1 V and the polarization time was 30 min. XPS results show that the passive film consisted by $Ni(OH)_2$ and $Ni_3(PO_4)_2$.

Keywords: Electroless Ni-P; Electrochemical impedance spectroscopy; Mott-Schottky; Passive film

1. INTRODUCTION

Electroless Ni-P coating (ENPC) has been the focus of considerable attention because of its good corrosion resistance, good wear resistance, and high hardness. The ENPC has been extensively used in many fields, such as the automotive, aerospace, computer, and electronics industries [1-3]. Ni-P alloys that contain high phosphorus (>12 wt.%) are considered to be in the amorphous state. Amorphous Ni-P alloys have higher corrosion resistance than pure nickel in acidic and neutral media [4, 5]. Many researchers have attributed better corrosion resistance to the amorphous structure, that is, to the lack of grain boundaries, dislocation, and inclusions of amorphous structures [4, 6-8]. However, sometimes, this amorphous theory cannot explain why crystallized Ni-P also showed better corrosion resistance [9]. Recently, more researchers generally agreed that the better corrosion resistance of high-

phosphorus coatings should be attributed to the inhibition of anode dissolution, the so-called passivation film theory. However, this theory is still the subject of debate [10-12].

Passivation film theory has been applied to explain some anticorrosion mechanism of alloys. Models of the formation and destruction of passive films have been established. Among these models, the point defect model (PDM) established by Macdonald and the solute-vacancy interaction model have been the subject of considerable interest. Based on passivation film theory, passive films possessing a bipolar characteristic show the best corrosion resistance, that is, the passive films can not only obstruct the positive ions out but also resist the negative ions in. In this situation, the protection rule of the passive films can be enhanced. This theory has been effectively used to explain the corrosion resistance of stainless steels [13-15].

Diegle et al.[16-18] have found that the Ni-P alloys can formed certain rich phosphorus passivity in corrosion solutions which means the passivation film theory may accommodate to the Ni-P coatings. However, few studies focused on the further study of the passive film formed upon amorphous Ni-P coating, such as the type of the passive film, the affect factors of the film, and the components of the film. In this study, we found that amorphous Ni-P coating can form passive films in certain conditions. Furthermore, electrochemical analyses were conducted to study the passive films. Characteristics of the passive films, such as semiconductor type and current carrier density, will be evaluated using the Mott-Schottky analysis. Different anodic potentials and polarization time were chosen to interpret the changing of the passive films. Contacting with the XPS analyses, it will be possible to explain the passive films components and corrosion mechanism in 5 wt. % sulfuric acid solution at ambient temperature.

2. EXPERIMENTAL

2.1 Preparation of the Ni-P coating

Substrates for electroless plating of Ni-P alloys, with a dimension of 10 mm × 10 mm × 1 mm and composed of low-carbon steel, were cleaned and polished before plating. The specimens were ground with SiC paper (grade 600) to ensure uniform surface roughness. Substrate pretreatment was conducted following a multistep process, which included alkaline cleaning, acid pickling, and sensitization. In this case, nickel sulfate was used as the nickel source and sodium hypophosphite solution was used as the reducing agent. Lactic acid and glycine were used as complexing agents. The samples were plated in an electroless bath for 4 h at 90 °C. The phosphorus content was 12.35 wt. % as tested by EDS.

2.2 XRD study

The phase structure of the coating was analyzed using X-ray diffraction (XRD; DX-2700) with Cu Kα radiation operated at 40 kV/30 mA. The scanning rate and scanning step were fixed at 1°/min, respectively.

2.3 Electrochemical test

Electrochemical measurements were conducted in 5 wt.% H_2SO_4 solution at ambient temperature through a classic three-electrode cell, in which the coating sample, Pt plate, and saturated calomel electrode (SCE) functioned as the working, counter, and reference electrodes, respectively. Then, the specimen was sealed with lacquer to leave only one surface (area = 1 cm^2) exposed to the corrosive medium. The working electrode was cleaned in acetone, agitated ultrasonically, and then rinsed with deionized water.

Prior to the electrochemical impedance spectroscopy (EIS) and polarization curve tests, open circuit potential (E_{OCP}) was measured for approximately 30 min until E_{OCP} was stabilized. The potentiodynamic polarization curves were recorded by scanning the electrode potential from -0.1 V versus SCE to 0.6 V at a scanning rate of 0.5 mV/s.

The passivation zone was determined based on the results of the potentiodynamic polarization curve. Then two schemes were chosen to obtain different passive films. First, three different anodic potentials (0.1 V, 0.2 V, and 0.3 V) were chosen from the passivation zone to form the passive films by potentiostatic tests for 60 min. Second, four different polarization time (15 min, 30 min, 60 min and 120 min) at 0.1 V were used to get four different passive films. Afterwards, the EIS test was used to interpret the corrosion mechanism of the passive films after undergoing the potentiostatic tests. EIS was conducted at scan frequencies that ranged from 100 kHz to 0.01 kHz. The amplitude of the applied sinusoidal signal was set to 10 mV on E_{OCP}. Results from the EIS test were presented as Nyquist and Bode plots. Equivalent circuits were established using the ZSimpWin software to fit the acquired data and evaluate the corrosion resistance.

The semiconductive properties of thin passive films formed on the Ni-P coating surface were determined using the doping density extracted from the Mott-Schottky plots. The Mott-Schottky analysis was conducted from -0.1 V to 0.5 V with a frequency and an amplitude of 1,000 Hz and 10 mV, respectively.

2.4 X-ray photoelectron spectroscopy (XPS) test

The XPS experiments were performed through an ESCALAB 250 (Thermo Fisher Scientific) X-ray photoelectron spectrometer. Photoelectron emission was excited by monochromatic Al Kα (1486.6 eV) source. The C1s peak from adventitious carbon at 248.8 eV was used as a reference to correct the charging shifts.

3. RESULTS AND DISCUSSION

3.1 Microstructure of the Ni-P coating

Figure 1 shows the XRD pattern of the as-plated Ni-P coating, which only a single broad profile was observed. This broad pattern indicates that the as-plated Ni-P coating has an amorphous structure.

The thickness of the electroless deposited Ni-P coating was greater than 40 μm after 4 h reaction in the plating solution. The thick layer helps reduce porosity on the surface of the as-plated Ni-P coating. Pores have an adverse effect on corrosion resistance through the corrosion reaction between the small pores and substrate. In this study, we assumed that no pores existed on the as-plated Ni-P coating with 40 μm thickness.

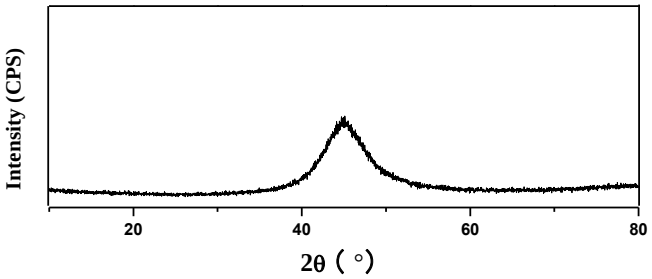

Figure 1. XRD pattern of electroless Ni-P alloy.

3.2 Potentiodynamic polarization

The potentiodynamic polarization curve of the as-plated Ni-P coating is shown in Fig. 2. The Ni-P coating was stabilized by treatment for 30 min in 5 wt. % H_2SO_4 solution before polarization testing.

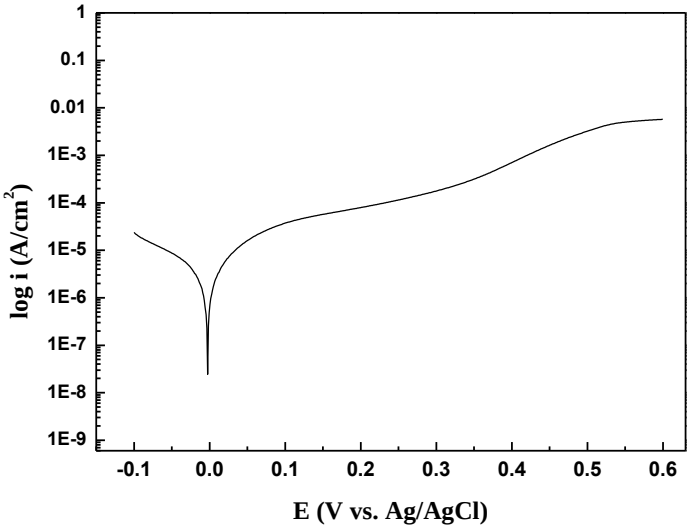

Figure 2. Polarization curve of Ni-P coating in 5 wt. % sulfuric acid solution.

As shown in Fig. 2, the anodic polarization curve has a narrow passive region from 0.1 V to 0.3 V. In this region, the current density is approximately 10^{-4} A/cm^2. When the potential reached to 0.4 V, the current density rapidly increased, which corresponds to the destruction of the passive film.

Besides, the electrochemical corrosion parameters can be obtained using the Tafel slopes. Results show that the I_{corr} is about 7.958 μA/cm^2 and the corrosion rate is 0.0925 mpy.

3.3 Influence of anodic potentials on the passive films

3.3.1 Electrochemical impedance spectroscopy

Figure 3 shows the EIS (electrochemical impedance spectroscopy) results of the passive films developed by potentiostatic polarization for 60 min at the selected anodic potentials of 0.1, 0.2, and 0.3 V, respectively.

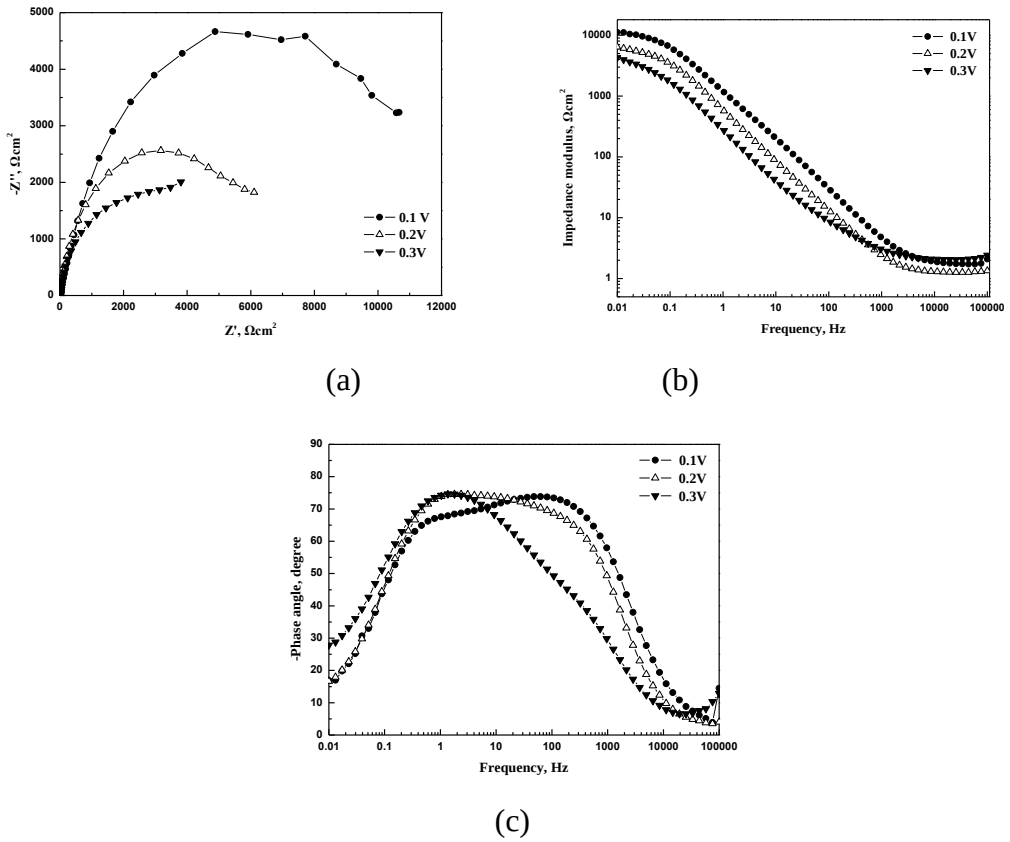

Figure 3. Impedance plots of the three passive films formed for 60 min at 0.1 V, 0.2 V and 0.3V on Ni-P surface in 5 wt. % sulfuric acid solution: (a) Nyquist plots; (b) frequency-absolute value plots; (c) frequency-angle plots.

Figure 3(a) shows the Nyquist plots of these passive films. All of these curves were similar, which comprised only one semicircle. However, the diameters of the semicircles were quite different. The diameter of the Nyquist plot determined the corrosion resistance of one material. This finding indicates that the as-plated amorphous Ni-P passivated under different anodic potentials have different corrosion resistance in 5 wt. % H_2SO_4 solution. The passive film formed on 0.1 V potential shows the largest capacitive loop, followed by the ones formed on 0.2 and 0.3 V potentials, respectively. These results indicate that the anodic potentials affect the films corrosion resistance. The result indicated that

corrosion resistance was improved when films were passivated in the following order of potentials: 0.1, 0.2, and 0.3 V.

The Bode plots of the passive films are shown in Fig. 3(b) and 3(c). Fig. 3(b) shows a single time constant in the plot of *f* versus$_{|Z|}$, and the curve of the 0.1 V potential is above the curves of 0.2 and 0.3 V potentials. This result indicates that the passive film developed at 0.1 V potential had the highest $_{|Z|}$ compared with other passive films. The highest $_{|Z|}$ means that the passive film at the potential of 0.1 V has the best anticorrosion property in the sulfuric acid corrosion medium, followed by passive films at potentials of 0.2 and 0.3 V. Fig. 3(c) shows a single-phase maximum angle in the plot of log*f* versus phase angle. Only a single time constant was observed during this process for the three curves.

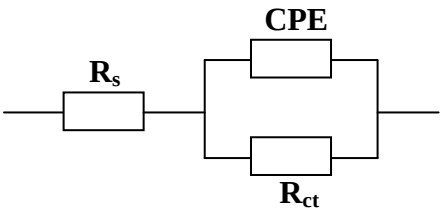

Figure 4. Equivalent circuit for simulating the EIS results.

The equivalent circuit was used to fit the Nyquist and Bode plots, as shown in Fig. 4[19-21]. The circuit comprised solution resistance (R_s), charge transfer resistance (R_{ct}), and double-layer capacitance (C_{dl}). R_{ct} can be used to evaluate the corrosion resistance of a system. A higher value of R_{ct} corresponds to better corrosion resistance. The double-layer capacitance provides information on the polarity and amount of charge at the film/solution interface. However, C_{dl} was replaced by a constant phase element (CPE) to represent the nonideal behavior caused by surface inhomogeneity [21]. Considering the deviation from the ideal dielectric behavior and surface homogeneities, the impedance of the CPE can be expressed as follows:

$$Z_{CPE} = Q(jw)^{-n}, \quad (1)$$

where Q is the admittance magnitude of CPE, w is the angular frequency, and n is the CPE power. The factor n is an adjustable parameter that always ranges between 0 and 1. The Z_{CPE} equals the pure resistor impedance when $n=0$. The Z_{CPE} equals the pure capacitance impedance when $n=1$. The fitted results are shown in Table 1.

Table 1. Fitted results for EIS spectra after 60 min potentiostatic tests under three anodic potentials (0.1 V, 0.2 V and 0.3V) on Ni-P surface in 5 wt. % sulfuric acid solution at room temperature.

Anodic potential V	R_s $\Omega \cdot cm^2$	CPE $\Omega^{-1} \cdot s^{-n} \cdot cm^{-2}$	n	R_{ct} $\Omega \cdot cm^2$
0.1	1.671	1.7×10^{-4}	0.8267	12230
0.2	1.228	3.45×10^{-4}	0.8436	6822
0.3	2.174	8.08×10^{-4}	0.7892	5516

The CPE and *n* values are related to the porosity and surface inhomogeneity of the passive films on the Ni-P coating surface [21]. As shown in Table 1, the CPE values of the three passive films show an increasing trend corresponding to the increasing anodic potentials (0.1 V to 0.3 V). Otherwise, the *n* values of the three passive films show a decreasing from 0.2 V to 0.1 V to 0.3 V potentials. These results indicate that the passive film formed at 0.1 V potential has less porosity and better surface homogeneity. The charge transfer resistance R_{ct} represents the corrosion resistance of the passive films. The film formed at 0.1 V potential has the highest R_{ct} value, which is almost twice of the other two films formed at 0.2 and 0.3 V potentials, respectively. This result indicates that the passive film developed at 0.1 V potential has the best corrosion resistance compared with the other two passive films in 5 wt. % sulfuric acid solution.

3.3.2 Mott-Schottky analysis

The Mott-Schottky method has been extensively used to characterize the semiconductive behavior of passive films, which can be achieved by measuring the space charge capacitance and Helmholtz capacitance under different applied potentials [22]. Based on Mott-Schottky theory, the capacitances of n-type and p-type semiconductors are shown in Eqs. (2) and (3), as follows:

$$C^{-2} = \frac{2}{\varepsilon\varepsilon_0 N_D e}\left(E - E_{fb} - \frac{kT}{e}\right), \quad (2)$$

$$C^{-2} = \frac{2}{\varepsilon\varepsilon_0 N_A e}\left(E - E_{fb} - \frac{kT}{e}\right), \quad (3)$$

where C is the measured capacitance of the film/electrolyte interface; ε_0 is the vacuum permittivity (8.854×10^{-14} F/cm); ε is the dielectric constant of the passive film; e is the electron charge (1.602×10^{-19} C); N_D and N_A are the donor and acceptor densities, respectively; E is the applied potential; E_{fb} is the flat-band potential; k is the Boltzmann constant (1.38×10^{-23} J/K); T is the absolute temperature; and the $\frac{kT}{e}$ is approximately 25 mV at room temperature (T = 298K).

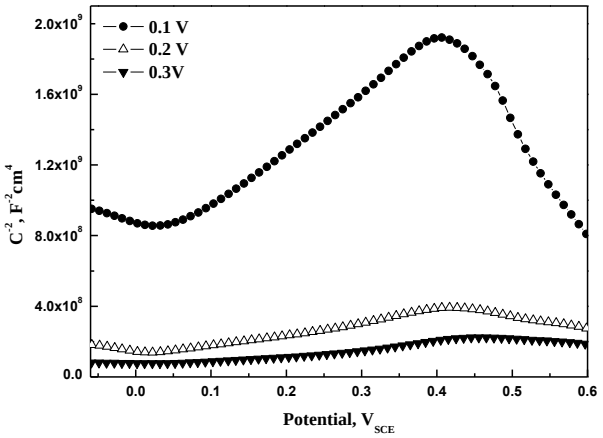

Figure 5. Mott-Schottky plots for the three passive films formed for 60 min at 0.1 V, 0.2 V and 0.3V on Ni-P surface in 5 wt. % sulfuric acid solution.

The semiconductor type of passive films can be determined using the slope of the Mott-Schottky plots at a certain potential region. If the slope has a positive value, then the passive film would be an n-type semiconductor. Otherwise, the passive film would be a p-type semiconductor. Plots of the three passive films formed at 0.1, 0.2, and 0.3 V potentials for 60 min in 5 wt. % H_2SO_4 solution are shown in Fig. 5. In the region of 0.1 V to 0.3 V, the three plots show a positive slope, which indicates that the passive films formed on as-plated amorphous Ni-P coatings in sulfuric acid solution are n-type semiconductors. The plot of the 0.1 V potential has a significantly inclined slope compared with the other two potentials.

Comparing the donor densities (N_D) of the three passive films can help us further understand the effect of the three anodic forced potentials. The donor densities N_D were calculated using Eq. (2) at the slopes between 0.1 V and 0.3 V in the Mott-Schottky plots. Results are shown in Table 2. As shown in Table 2, the values of N_D augmented with increasing the forced potentials. When the forced potential was 0.1 V, the donor density N_D had the lowest value, which was 4.702×10^{21} cm^{-3}. As a comparison, the N_D had the highest value of 4.537×10^{22} cm^{-3} when the forced potential increased to 0.3 V, which was approximately 10 times than that of the 0.1 V N_D value. Based on PDM theory, the electron donors are mainly oxygen vacancies and cation interstitials [22], whose density characterizes the pit nucleation ability. The higher the donor density, the easier the passive film will break. Based on N_D values shown in Table 2, we can infer that the corrosion resistance rates of the three passive films are significantly different. Corrosion resistance of the passive films decreased with the increasing in potentials from 0.1 V to 0.3 V. Moreover, the passive film formed at 0.1 V potential has more uniform internal structure and less porosity density. This helps to provide the protection to the matrix in acid solution at room temperature.

Table 2. The calculated donor densities (N_D) of the three passive films formed for 60 min at 0.1 V, 0.2 V and 0.3V on Ni-P surface in 5 wt. % sulfuric acid solution.

Passive potential V	N_D cm^{-3}
0.1	4.702E21
0.2	1.997E22
0.3	4.537E22

To further understand the affection of potentials on the passive films, Fig. 6 shows the variation of passive current and the time at different anodic potentials. It shows that the passive current increased with the anodic potentials enlarged. Due to the impurities in passive films can be thought to be the charged ions to participate in electric conduction, higher current means more impurities. The impurities can reduce the protection of the passive film. So, the passive film formed at 0.1 V has the best protection to the matrix compared to the other two ones. This result corresponds to the upper EIS results.

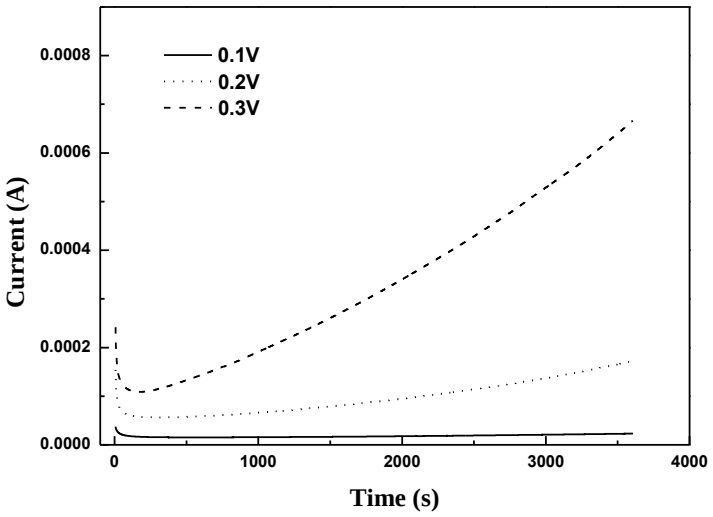

Figure 6. Current-time curves of the three passive films formed for 60 min at 0.1 V, 0.2 V and 0.3V on Ni-P surface in 5 wt. % sulfuric acid solution.

3.4 Influence of polarization time on the passive films

3.4.1 Electrochemical impedance spectroscopy

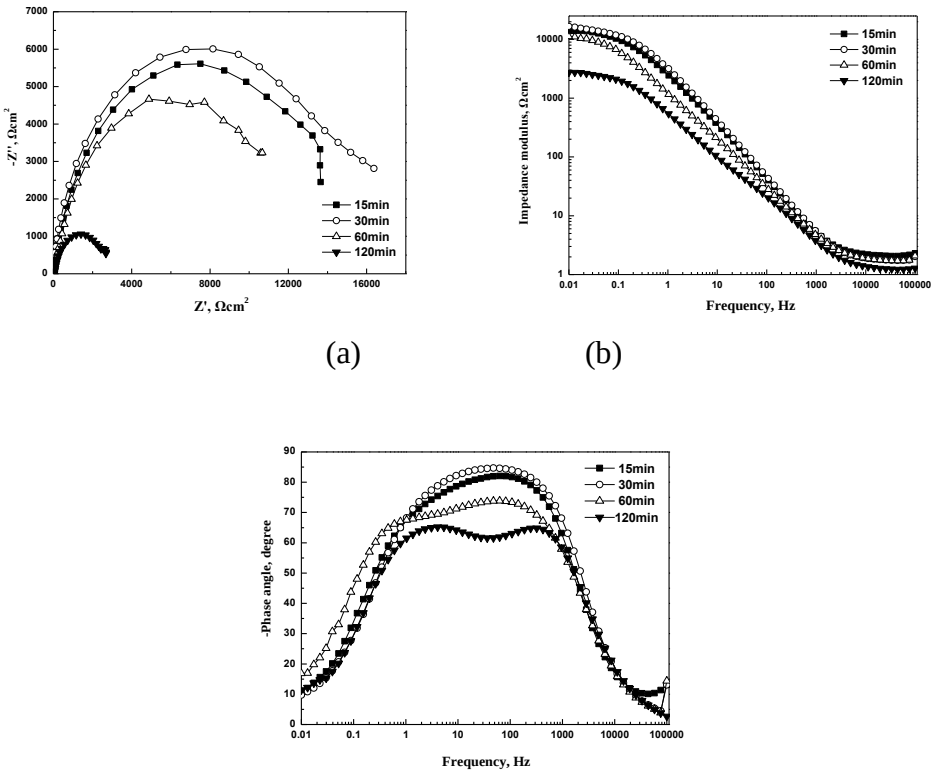

(a) (b)

(c)

Figure 7. Impedance plots of four polarization time films at 0.1V potential in 5 wt. % sulfuric acid solution: (a) Nyquist plots; (b) frequency-absolute value plots; (c) frequency-angle plots.

Figure 7 shows the EIS (electrochemical impedance spectroscopy) results of the passive films developed by potentiostatic polarization for 15 min, 30 min, 60 min and 120 min at 0.1V, respectively. Fig. 7(a) shows the Nyquist plots of these passive films. All of these curves were comprised by one semicircle. The passive film formed after 30 min shows the largest capacitive loop, followed by the ones formed after 15 min, 60 min and 120 min, respectively. When the passive time reached to 120 min, the capacitive loop became much smaller than the others. These results indicate that the polarization time can also affect the corrosion resistance of the passive films. Besides, the corrosion resistance tendency of the four passive films is increased at first and then decreased, which can be arrayed in the following order through passive times: 30, 15, 60 and 120 min.

The Bode plots of the passive films are shown in Fig. 7(b) and 7(c). Fig. 7(b) shows a single time constant in the plot of *f* versus $|Z|$, and the curve of the 30 min is above the curves of 15 min, 60 min and 120 min. This indicates that the passive film developed after 30 min has the highest value of $|Z|$. The highest $|Z|$ means the passive film forming after 30 min at 0.1 V has the best anticorrosion property in the sulfuric acid solution. By contrast, the passive film forming after 120 min has the worst corrosion resistance among the four passive films. Fig. 7(c) shows a single-phase maximum angle in the plot of log*f* versus phase angle. The angles of the 15 min and 30 min passive films which have the narrow peaks are approximately 90° indicating a pure capacitive behavior, which means the two passive films are more stable than the other two ones. When the passive time reached to 60 min, the shape of the peak became a broad peak and the angles became smaller. This means the passive film began to be destroyed. When the passive time extended to 120 min, the angle value decreased and the broad single peak changed to a broad double peak, this means the passive film formed on the surface of Ni-P coating was destroyed, some matrix exposed in the corrosive solution.

Table 3. Fitted results for EIS spectra of four polarization time films at 0.1 V potential in 5 wt. % sulfuric acid solution at room temperature.

Passive time min	R_s $\Omega \cdot cm^2$	CPE $\Omega^{-1} \cdot s^{-n} \cdot cm^{-2}$	n	R_{ct} $\Omega \cdot cm^2$
15	2.034	7.21×10^{-5}	0.9016	13760
30	1.745	5.32×10^{-5}	0.9344	14880
60	1.671	1.7×10^{-4}	0.8267	12230
120	1.117	3.96×10^{-4}	0.7595	3033

The equivalent circuit was shown in Fig. 4. And the fitted results are shown in Table 3. As shown in Table 3, with the polarization time increased, the *n* values of passive films first increased and decreased later. When the polarization time was 30 min, the passive film has the highest n value (very close to 1), which means this passive film has less porosity and better surface homogeneity. Meanwhile, the 30 min passive film also has the highest value of R_{ct} indicating this passive film has the best corrosion resistance compared with the other three passive films formed at 0.1 V in 5 wt. % sulfuric acid solution.

3.4.2 Mott-Schottky analysis

Figure 8 shows the Mott-Schottky plots of four passive films in 5 wt. % H_2SO_4 solution, which formed at 0.1 V for 15 min, 30 min, 60 min and 120 min, respectively. The plots tendency is the same as Fig. 6.

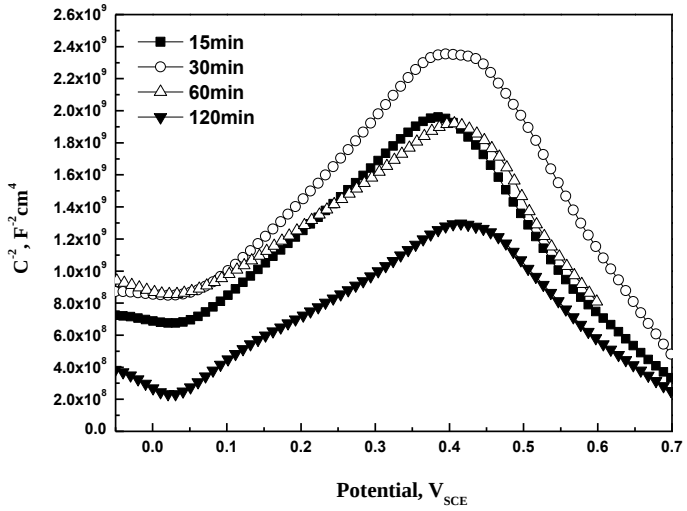

Figure 8. Mott-Schottky plots of the four different passive time films at 0.1 V potential in 5 wt. % sulfuric acid solution.

The four curves show the same positive slope, which indicates that the four passive films are n-type semiconductors. Besides, the curve shows the maximum slope when the passive time was 30 min. When the passive time was 15 min and 60 min, the two curves have almost the same slope and smaller than the 30 min one. When the passive time reached to 120 min, the curve has the minimum slope. This means polarization time is another important factor in the passive films semi-conductor properties. The polarization time can affect the internal components of the passive films. For further discussion, the donor densities N_D were calculated using Eq. (2) and the results are shown in Table 4. As shown in Table 4, when the polarization time was 15 min, the donor density N_D was 3.182×10^{21} cm^{-3}. When the polarization time reached to 30 min, the donor density N_D had the lowest value, which was 2.429×10^{21} cm^{-3}. This means the passive film formation is more complete during this process. The passive film obtained more density internal structure and less porosity density during this time. However, when the polarization time extended to 60 min and 120 min, the N_D values increased to 3.739×10^{21} cm^{-3} and 4.278×10^{21} cm^{-3}, respectively. This means the passive film has begun to be destroyed. Higher donor density represents looser structure and more porosity. Then the protective result of passive film also reduced. The further reason would be discussed through the XPS test. Above all, the polarization time is not good as long as possible for the amorphous Ni-P plating under sulfuric acidic environment. When the polarization time was 30 min at 0.1 V, the passive film has the best protection to the matrix.

Table 4. The calculated donor densities (N_D) of the four passive films at 0.1 V potential in 5 wt. % sulfuric acid solution.

Passive time min	N_D cm^{-3}
15	3.182E21
30	2.429E21
60	3.739E21
120	4.278E21

3.5 XPS analysis of the passive film

In general, both composition and structure of the passive film can affect the semi-conductor properties. The structure of the passive film has been discussed as above mentioned; otherwise, it is necessary to clarify the chemical compositions of the passive film. The passive film formed at 0.1 V for 30 min in sulfuric acidic solution was examined by X-ray photoelectron spectroscopy.

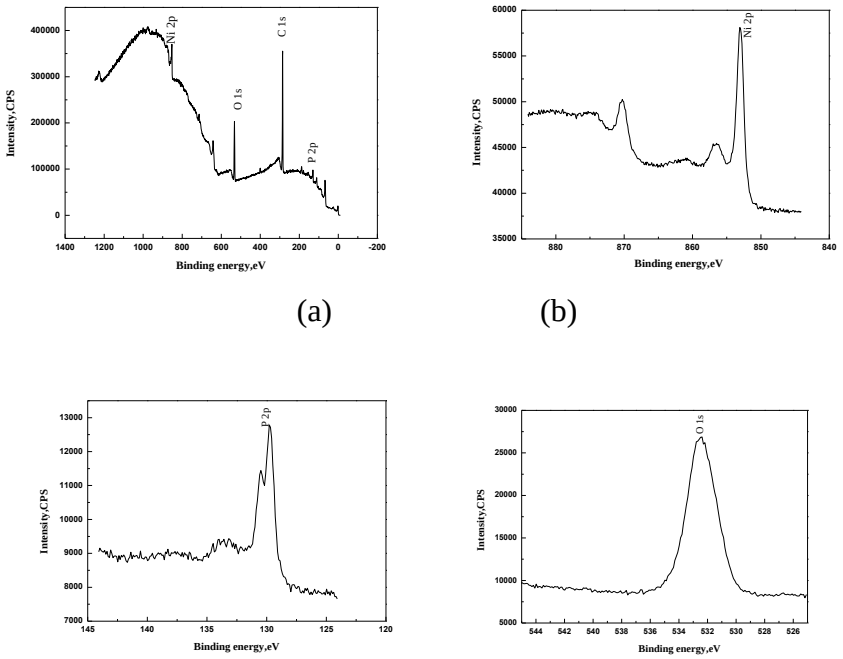

Figure 9. XPS spectrum of the passive film formed on surface of amorphous Ni-P coating in 5 wt. % sulfuric acid solution: (a) wide spectrum; (b) Ni2p; (c) P2p; (d) O1s.

Figure 9 presents XPS spectrum and three main elements characteristic peaks of the passive film on the Ni-P surface. As shown in Fig.9 (a), the passive film mainly contains three elements: Ni, P and O. Fig.9 (b) shows the scan spectra of Ni2p, this spectra can be separated into three peaks: 870.27 eV、856.47 eV and 853.03 eV, respectively, contributing to NiO, $Ni(OH)_2$ and Ni_2O_3[23-25]. Fig.9 (c) shows the scan spectra of P2p, this spectra can be separated into two peaks: 130.50 eV and 129.71 eV, contributing to（PO_4^{-3}）and P[26, 27]. Fig.9 (d) shows the spectra of O1s, compared with the

standard binding energy of O, it can infer that the element O exists in O^{2-} form. Through the combination of the above analysis, a preliminary estimate about the composition of the passive films can obtain. The passive films should be made up by NiO, $Ni(OH)_2$, Ni_2O_3, and $Ni_3(PO_4)_2$.

Further analyses are as follows. NiO is an alkaline oxide; it can easily be dissolved in acids. So, it should be excluded from the results. The other oxide Ni_2O_3, should also be excluded because it can also be dissolved in sulfuric acid and produce oxygen. For the passive film still holds metallic luster, this means the surface passive films are dense and stable. Considering the previous research results[28, 29], the passive film should contain some $Ni(OH)_2$. In this acid solution corrosion experiment, the dissolving speed of $Ni(OH)_2$ is faster than the $Ni_3(PO_4)_2$. With the proceed of this experiment, the amount of $Ni_3(PO_4)_2$ was increasing gradually, while the $Ni(OH)_2$ was decreasing. The protection effect of $Ni_3(PO_4)_2$ is poor than the $Ni(OH)_2$. So, with the increasing of $Ni_3(PO_4)_2$ and the decreasing of $Ni(OH)_2$, the density of the passive films was reducing, besides, the corrosion resistance of the Ni-P surface passive film was decreasing. This can be used to explain the polarization time affection on the passive film as discussed in 3.4.2. Above all, it can be deduced that the passive films formed in acid solution are mainly consist by $Ni(OH)_2$ and $Ni_3(PO_4)_2$. This film helps to improve the corrosion resistance of the electroless Ni-P coating in acid solution.

According to the changing elements and the corrosion products of the coating, the possible corrosion mechanism of electroless Ni-P coating are listed below.

There resists solubility equilibrium on the Ni-P coating surface: $Ni \rightleftharpoons Ni^{2+}(ads) + 2e$

The forming mechanism of $Ni(OH)_2$: $Ni^{2+} + 2H_2O \rightarrow Ni(OH)_2 + 2H^+$

The forming mechanism of $Ni_3(PO_4)_2$: $P + 2H_2O \rightarrow H_2PO_2^- + 2H^+ + e^-$; $H_2PO_2^- + O_2 + H^+ \rightarrow H_3PO_3$; $3Ni^{2+} + 2PO_3^{3-} + O_2 \rightarrow Ni_3(PO_4)_2$

In conclusion, $Ni(OH)_2$ and $Ni_3(PO_4)_2$ concentrated on the coating surface, this was beneficial to prevent further corrosion process.

4. CONCLUSIONS

1. The high-phosphorus content Ni-12.35 wt. % P coatings undergo the passivation process in 5 wt. % sulfuric acid solution. The corrosion resistance of passive films obtained on the surface of Ni-P coatings affect by anodic potentials and polarization time. When the anodic potential was 0.1 V and polarization time was 30 min, the passive film showed the best corrosion resistance.

2. The passive films on the Ni-P coatings possess the n-type semiconductor characteristic based on the Mott-Schottky analysis. Moreover, the donor density N_D for the passive film passivated at anodic potential of 0.1 V and polarization time of 30 min had the lowest value, which means that this passive film has the best densification and stability.

3. XPS analysis results show that the passive film formed on the amorphous Ni-P surface in 5 wt.% sulfuric acid solution was consisted by $Ni(OH)_2$ and $Ni_3(PO_4)_2$.

ACKNOWLEDGEMENTS
This project is supported by National Natural Science Foundation of China (No. 51271099).

References

1. S. Mu, N. Li, D. Li, L. Xu, *Applied Surface Science*, 256 (2010) 4089.
2. H. Ashassi-Sorkhabi, S.H. Rafizadeh, *Surface and Coatings Technology*, 176 (2004) 318.
3. M. Palaniappa, G.V. Babu, K. Balasubramanian, *Materials Science and Engineering: A*, 471 (2007) 165.
4. H. Habazaki, S.-Q. Ding, A. Kawashima, K. Asami, K. Hashimoto, A. Inoue, T. *Masumoto, Corrosion Science*, 29 (1989) 1319.
5. Y.F. Shen, W.Y. Xue, Z.Y. Liu, L. Zuo, *Surface and Coatings Technology*, 205 (2010) 632.
6. G. Lu, G. Zangari, *Electrochimica Acta*, 47 (2002**)** 2969.
7. A. Królikowski, B. Karbownicka, O. Jaklewicz, *Electrochimica Acta*, 51 (2006) 6120.
8. A. Królikowski, P. Butkiewicz, *Electrochimica Acta*, 38 (1993) 1979.
9. T. Mimani, S.M. Mayanna, *Surface and Coatings Technology*, 79 (1996) 246.
10. H. Tsuchiya, S. Fujimoto, O. Chihara, T. Shibata, *Electrochimica Acta*, 47 (2002) 4357.
11. D.-S. Kong, S.-H. Chen, C. Wang, W. Yang, *Corrosion Science*, 45 (2003) 747.
12. M.J. Carmezim, A.M. Simões, M.F. Montemor, M.D. Cunha Belo, *Corrosion Science*, 47 (2005) 581.
13. A. Fattah-alhosseini, M.A. Golozar, A. Saatchi, K. Raeissi, *Corrosion Science*, 52 (2010) 205.
14. A. Fattah-alhosseini, F. Soltani, F. Shirsalimi, B. Ezadi, N. Attarzadeh, *Corrosion Science*, 53 (2011) 3186.
15. R.M. Fernández-Domene, E. Blasco-Tamarit, D.M. García-García, J. García-Antón, *Thin Solid Films*, 558 (2014) 252.
16. R.B. Diegle, C.R. Clayton, Y. Lu, N.R. Sorensen, *Journal of the Electrochemical Society*, 134 (1987) 138.
17. H. Habazaki, S.Q. Ding, A. Kawashima, K. Asami, K. Hashimoto, A. Inoue, T. *Masumoto, Corrosion Science*, 29 (1989) 1319.
18. J. Flis, D.J. Duquette, *Journal of the Electrochemical Society*, 131 (1984) 34.
19. J.N. Balaraju, V.E. Selvi, V.K.W. Grips, K.S. Rajam, *Electrochimica Acta*, 52 (2006) 1064.
20. Z. Yin, F. Chen, *Surface and Coatings Technology*, 228 (2013) 34.
21. M. Alishahi, S.M. Monirvaghefi, A. Saatchi, S.M. Hosseini, *Applied Surface Science*, 258 (2012) 2439.
22. J. Ding, L. Zhang, M. Lu, J. Wang, Z. Wen, W. Hao, *Applied Surface Science*, 289 (2014) 33.
23. E.E. Khawaja, M.A. Salim, M.A. Khan, F.F. Al-Adel, G.D. Khattak, Z. Hussain, *Journal of Non-Crystalline Solids*, 110 (1989) 33.
24. A.N. Mansour, *Surface Science Spectra*, 3 (1994) 221.
25. K. Kishi, *Journal of Electron Spectroscopy and Related Phenomena*, 46 (1988) 237.
26. R. Franke, T. Chasse, P. Streubel, A. Meisel, *Journal of Electron Spectroscopy and Related Phenomena*, 56 (1991) 381.
27. C.J. Powell, *Journal of Electron Spectroscopy and Related Phenomena*, 185 (2012) 1.
28. M.C. Oliveira, A.M. Botelho do Rego, *Journal of Alloys and Compounds*, 425 (2006) 64.
29. A. Machet, A. Galtayries, S. Zanna, L. Klein, V. Maurice, P. Jolivet, M. Foucault, P. Combrade, P. Scott, P. Marcus, *Electrochimica Acta*, 49 (2004) 3957